IOPscience iopscience.iop.org

Home Search Collections Journals About Contact us My IOPscience

Thermodynamic properties of magneto-anisotropic nanoparticles

This article has been downloaded from IOPscience. Please scroll down to see the full text article.

2009 J. Phys.: Condens. Matter 21 236003

(http://iopscience.iop.org/0953-8984/21/23/236003)

View the table of contents for this issue, or go to the journal homepage for more

Download details:
IP Address: 129.252.86.83
The article was downloaded on 29/05/2010 at 20:09

Please note that terms and conditions apply.

J. Phys.: Condens. Matter **21** (2009) 236003 (9pp) doi:10.1088/0953-8984/21/23/236003

# Thermodynamic properties of magneto-anisotropic nanoparticles

**Malay Bandyopadhyay**

Department of Theoretical Physics, Tata Institute of Fundamental Research, Colaba, Mumbai 400005, India

E-mail: malay@theory.tifr.res.in

Received 24 September 2008, in final form 3 March 2009
Published 7 May 2009
Online at stacks.iop.org/JPhysCM/21/236003

**Abstract**

The purpose of this paper is to study the thermodynamic equilibrium properties of a collection of non-interacting three-dimensional (3D) magnetically anisotropic nanoparticles in the light of classical statistical physics. Pertaining to the angular dependence ($\alpha$) of the magnetic field with the anisotropy axis, energy landscape plots are obtained which reveal a continuous transition from a double well to a single well for $\alpha = \frac{\pi}{2}$ and show an asymmetric bistable shape for other values of $\alpha$. The present analysis is related to the interpretation of equilibrium magnetization and static susceptibility of a nanomagnetic system as a function of external magnetic field, $B$, and temperature, $T$. The magnetization and susceptibility confirm the non-Langevin behaviour of magneto-anisotropic monodomain particles. The susceptibility analysis establishes the ferromagnetic-, antiferromagnetic- and paramagnetic-like coupling for various $\alpha$. This study reveals the essential role of magneto-anisotropic energy in the interpretation of the magnetic behaviour of a collection of non-interacting single-domain nanoparticles.

(Some figures in this article are in colour only in the electronic version)

## 1. Introduction

Nanometre-sized magnetic particles have provoked immense interest in both the scientific as well as the technological arenas [1–5]. The development of intense fabrication techniques helps in the preparation of nanoparticles with satisfactory structural and chemical properties. The study and analysis process gained acceleration due to the exaggerating growth of measurement facilities like magnetic force microscopy [6], micro-SQUIDS [7] and other magnetometry measurements [8, 9]. Such techniques have led to the measurement of the magnetization process of single magnetic clusters in nanometre scales.

The magnetic moment of the nanoparticle consists of the single-domain structure of ferromagnetic spins with a large net spin, $S$ ($\sim 10^3$–$10^4$) and hence it is called a supermoment [10–12]. This spin couples with a large number of environmental degrees of freedom of the host material. Dynamical disturbances of the surrounding environment lead to a rotational Brownian motion of the large spin surmounting the magnetic-anisotropy potential barriers [13, 14]. In the high barrier limit, the magnetic response of the non-interacting single-domain particles follow the Néel relaxation process with the relaxation time $\tau$ characterized by the relation

$$\tau = \tau_0 \exp\left(\frac{\Delta E_a}{k_B T}\right), \tag{1}$$

where $\tau_0 \sim 10^{-10}$–$10^{-13}$ s. Here $\tau_0$ is related to the intra-well motion and the height of the energy barrier due to anisotropy is $\Delta E_a = KV$, where $K$ is the anisotropy constant, $V$ is the particle volume, $k_B$ is the Boltzmann constant and $T$ denotes the absolute temperature. Depending on the relation of $\tau$ with the measurement time $t_m$, various interesting phenomena can be observed. For $\tau \ll t_m$, the magnetic moment exhibits the thermal equilibrium distribution of a paramagnet. For $\tau \gg t_m$, the magnetic moment stays very close to the energy minima as the reversal mechanism is blocked. For $\tau \sim t_m$, nonequilibrium phenomena, i.e. magnetic relaxation, is observed. In this work, all discussions are concentrated in the thermal equilibrium regime where $\tau \ll t_m$. In this context, the classical Stoner–Wohlfarth (SW) simplistic uniform rotation model of a giant magnetic vector really provides an insightful and realistic picture of magnetization reversal of single-domain nanoparticles [15]. Here, we follow the same kind of arguments as proposed by Stoner and Wohlfarth [15].

 © 2009 IOP Publishing Ltd Printed in the UK

The first study on the superparamagnetic behaviour of an aligned assembly of uniaxially anisotropic particles was made by West [16]. Further investigations regarding possible configurations encountered in experiment was made by Müller and Thurley [17]. Deviations from classical Langevin theory were demonstrated by several authors [18–23]. Madsen *et al* have studied the effect of anisotropic energy on the interpretation of magnetization data for antiferromagnetic particles [24]. Vargas *et al* depict a second-order phase transition in non-interacting magneto-anisotropic nanoparticles when the external magnetic field is applied perpendicular to the anisotropy axis with the order parameter being the magnetization parallel to the field [25, 26]. Magneto-caloric properties of non-interacting magneto-anisotropic nanoparticles have been studied in [29].

In this work, we investigate the effect of magneto-anisotropic energy on the equilibrium thermodynamic properties of fine particles. By thermal equilibrium behaviour, we mean that the measurement or observation time, $t_m$, is much larger than the characteristic relaxation time, $\tau$, of the system, i.e. we restrict our discussion to the regime $t_m \gg \tau$. On the other hand, below a certain critical size (for Fe, it is 150 nm), it is not energetically favourable to form a domain wall and the particle is said to be a monodomain or fine-particle system [11]. Having explained the terms 'equilibrium properties' and 'fine particles', we are now ready to describe briefly our findings. Variations in the angle between the anisotropy axis and the external magnetic field, $\alpha$, and between the former and the magnetic moment, $\theta$, give deep insights into the thermodynamic equilibrium properties of magneto-anisotropic nanoparticles. We have extended the study of Vargas *et al* [25, 26] by choosing the magnetic moment and the anisotropy field vectors to be independent and arbitrary. On the other hand, Vargas *et al*, restricted their study to the particular case in which the external field is perpendicular to the anisotropy axis. Also, we consider the particle size distribution of nanoparticles rather than the case of identical non-interacting particles as studied by Vargas *et al* [25, 26]. Thus the present study is much more realistic and close to the experimental realizations [27, 4, 28].

The variation of the magnetization and susceptibility with respect to external parameters like external field, $B$, and temperature, $T$, is extensively studied. The effect of anisotropy is evident from the magnetization versus reduced magnetic field, $\xi$, curve. The variation of inverse susceptibility with temperature for different angles, $\alpha$, shows paramagnetic-, ferromagnetic- and antiferromagnetic-like coupling which clearly exhibits the effect of magneto-anisotropic energy on the static susceptibility of nanomagnetic systems.

With the preceding background, the rest of this paper is organized as follows. In section 2, we discuss the model system and other basic considerations about this model system. Section 3 deals with the model Hamiltonian and the relevant thermodynamic functions. In section 4.1, the energy landscape for the nanomagnetic system as a function of $\alpha$ is explored. The variation of equilibrium angle, $\theta$, with dimensionless reduced magnetic field, $h$, for different $\alpha$ is demonstrated in section 4.2. Section 5 deals with the variation of magnetization and susceptibility with respect to $\xi$ and $T$. Finally, the paper is concluded in section 6.

## 2. Model and basic considerations

In this section, we discuss our model and some basic considerations which one needs to study the thermodynamic equilibrium properties of single-domain particles. Kittle has shown that, below a critical size, domain wall formation is energetically unfavourable [11]. These kinds of particles are called single-domain particles. In the absence of an external magnetic field, a bulk ferromagnet may have no net magnetization due to the cancellation from different domains. But a single domain particle acts as a giant magnetic moment and the magnetic moment per particle depends on the particle volume and the number of atoms it has. Throughout this paper, we concentrate on the thermodynamic properties of a collection of such monodomain particles which are dispersed in a solid matrix [30, 31]. Further, we restrict our study to mathematically tractable systems with axially symmetric magneto-anisotropy. But it provides valuable insights into more complex situations. All our considerations are based on the Stoner–Wohlfarth model for single-domain particles [15]. In this model, all spins within the particle are aligned due to exchange interaction and this is the dominating magnetostatic effect within the particle. The giant magnetic moment direction fluctuates, because the anisotropy energy is comparable to thermal energy. The direction of the moment is determined by the net anisotropy of the system and the energy is minimized. This magnetization reversal process occurs by coherent rotation, i.e. the atomic spins remain parallel to each other as they rotate to a new direction [13, 14]. Here, we are considering ideal monodomain particles in which other more complex interactions both within the particles and between the particles are neglected. Thus, our system has only magnetocrystalline energy and Zeeman energy due to the interaction with an external field.

Now, we need to specify the validity of this model, especially in which temperature range it is valid. To specify this temperature range, we follow the arguments given by Garcìa-Palacios [20]. It has already been mentioned that the thermal equilibrium behaviour of ideal monodomain particles with uniaxial anisotropy is observed when $t_m \gg \tau$. From equation (1), one can easily understand that thermal equilibrium behaviour exists when the anisotropic potential barrier, $\Delta E_a$, is much larger than the thermal energy, $k_B T$. Besides, the 'high barrier' regime, equation (1), still holds down to $\Delta E_a/k_B T \geqslant 2$. It is known that $\tau_0$ for magnetic nanoparticles is $\sim 10^{-10}$–$10^{-12}$ s. Thus, the thermal equilibrium range for a given measurement time, $t_m$, is given by $\ln(\frac{t_m}{\tau_0}) > \Delta E_a/k_B T \geqslant 0$. For magnetic measurements, $t_m \sim$ 1–100 s and the thermal equilibrium range is quite wide $25 > \Delta E_a/k_B T \geqslant 0$. So, the frequently encountered statement that the thermal equilibrium behaviour occurs when $\Delta E_a \geqslant k_B T$ is needlessly constrictive. For example, if $t_m = \tau_0 10^{12}$ (a typical value for magnetic measurements), one finds that $\Delta E_a/k_B T \simeq 27.6$. For $\Delta E_a/k_B T = 25$, one can obtain $\tau = 0.08 t_m$. Thus, the system is in thermal equilibrium, but $\Delta E_a$ is still much larger than $k_B T$ [20].

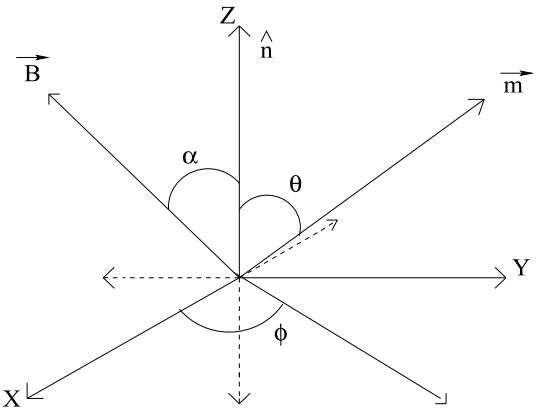


**Figure 1.** Coordinate system showing the unit vector along the anisotropy axis, $\hat{n}$, the external magnetic field vector, $\vec{B}$, and the magnetic moment vector, $\vec{m}$, along with the angles $\alpha$, $\theta$ and $\phi$ as referred to in the text.

## 3. Hamiltonian and other relevant quantities

We consider a collection of non-interacting single-domain magnetic particles. In a single-domain particle, nearly $10^5$ magnetic moments are coherently locked together in a given direction, thus yielding a supermoment. In this nanomagnetic system, every particle consists of a single magnetic domain with all its atomic moments rotating coherently and resulting in a constant absolute value of magnetization $m = m_s V$, where $V$ is the volume of the particle and $m_s$ is the saturation magnetization which is supposed to be independent of particle volume and temperature. In our system, the Hamiltonian consists of two parts, one representing the Zeeman energy and the other is the anisotropic energy (due to the crystalline structure of the particle). For the sake of simplicity, we consider a temperature-independent uniaxial anisotropy. Denoting the external applied magnetic field as $\vec{B}$, the Hamiltonian is given by

$$\mathcal{H}(\vec{m}) = -\frac{KV}{m^2}(\vec{m}\cdot\hat{n})^2 - \vec{m}\cdot\vec{B}, \tag{2}$$

where $\hat{n}$ is a unit vector along the anisotropy axis, $\vec{m}$ is the magnetic moment of the single-domain particle and $\vec{B}$ is the direction of the external magnetic field, as shown in figure 1, and $K$ is the anisotropy constant. This model is valid only if the exchange interaction strength of the system is much larger than $K$ and $B$. Now denoting $(\theta, \phi)$ and $(\alpha, 0)$ as the angular coordinates of $\vec{m}$ and $\vec{B}$, respectively, and choosing $\hat{n}$ as the polar axis of the spherical polar coordinate system, one can write the total magnetic potential in the form as follows:

$$-\beta\mathcal{H} = \sigma\cos^2\theta + \xi_\parallel\cos\theta + \xi_\perp\sin\theta\cos\phi, \tag{3}$$

where $\sigma = \frac{KV}{k_B T}$, $\xi_\parallel = \xi\cos\alpha$, $\xi_\perp = \xi\sin\alpha$, $\xi = \frac{mB}{k_B T}$, $\beta = \frac{1}{k_B T}$, $k_B$ is the Boltzmann constant and $T$ is the temperature of the system. One can rewrite equation (3) as follows:

$$\mathcal{H}_{\text{eff}} = -\frac{\beta\mathcal{H}}{\sigma} = \cos^2\theta + 2h(\cos\alpha\cos\theta + \sin\alpha\sin\theta\cos\phi), \tag{4}$$

with $h = \frac{\xi}{2\sigma}$. Expressions for the magnetization curve where anisotropy is included have been discussed by [18–21]. This calculation is based on the theory of Hanson *et al* [18] and Respaud [21]. For a uniaxial anisotropic nanomagnetic system, the anisotropy energy depends only on the angle between the magnetization and the direction of easy magnetization in the particle, $\theta$. In thermal equilibrium, the magnetization in the direction of $\vec{m}$ is proportional to the Boltzmann factor for a fixed orientation of the easy axis:

$$f(\hat{m}) = z^{-1}\exp[\sigma(\hat{m}\cdot\hat{n})^2 + \xi(\hat{m}\cdot\hat{h})], \tag{5}$$

where $\hat{m}$, $\hat{h}$ are the unit vectors along the direction of the magnetic moment and the external magnetic field, and $z$ is the partition function defined by

$$z = \int \exp[(\hat{m}\cdot\hat{n})^2 + 2h(\hat{m}\cdot\hat{h})]. \tag{6}$$

Thus, we have

$$\hat{m}\cdot\hat{h} = \cos\lambda = \sin\alpha\sin\theta\cos\phi + \cos\alpha\cos\theta \tag{7}$$

$$\hat{m}\cdot\hat{n} = \cos\theta. \tag{8}$$

Using the Boltzmann statistics, the expectation value of the reduced magnetization with a given orientation of the easy axis is given by

$$m(\alpha) = \frac{M}{m_s} = \langle\cos\lambda\rangle = \frac{\int_0^{2\pi}\mathrm{d}\phi\int_0^{\pi}\cos\lambda\mathrm{e}^{-\mathcal{H}_{\text{eff}}}\sin\theta\,\mathrm{d}\theta}{\int_0^{2\pi}\mathrm{d}\phi\int_0^{\pi}\mathrm{e}^{-\mathcal{H}_{\text{eff}}}\sin\theta\,\mathrm{d}\theta}. \tag{9}$$

None of the integrations in equation (9) is doable analytically. However, equation (9) can be simplified by using the modified Bessel functions and performing the analytic integration over $\phi$. Thus, the magnetization of such a collection of non-interacting identical particles aligned with an angle $\alpha$ with respect to $B$ is given by

$$m(\alpha) = \frac{N(\alpha)}{D(\alpha)}, \tag{10}$$

with

$$N(\alpha) = \int_0^{\pi}\mathrm{d}\theta\sin\theta\exp(2h\cos\lambda + \cos^2\theta) \times [\sin\alpha\sin\theta I_1(2h\sin\alpha\sin\theta) + \cos\alpha\cos\theta I_0(2h\sin\alpha\sin\theta)], \tag{11}$$

$$D(\alpha) = \int_0^{\pi}\mathrm{d}\theta\sin\theta\exp(2h\cos\lambda + \cos^2\theta) \times I_0(2h\sin\alpha\sin\theta), \tag{12}$$

where $I_0$ and $I_1$ are the modified Bessel functions of order 0 and 1, respectively. Considering a random distribution of anisotropy axes one can show

$$M_B(h) = \tfrac{1}{2}\int_0^{\pi}\mathrm{d}\alpha\sin\alpha m(\alpha). \tag{13}$$

However, there will be a distribution of particle sizes in any real fine-particle system. The existence of particle size distribution can be taken into account by taking an average over the full

particle size distribution. Thus, the magnetization of such a system with a distribution of particle sizes consists of the sum of contributions from the superparamagnetic and the blocked particles. The weightage of these two is maintained by the size distribution function of the particles, $f(y)$. Now, the magnetization for this polydispersive system is given by

$$M_{\rm Pol} = \int_0^{y_{\rm sp}} M_{\rm sp}(y,h) f(y)\,{\rm d}y + \int_{y_{\rm sp}}^{\infty} M_{\rm B}(h) f(y)\,{\rm d}y, \quad (14)$$

where $y$ is the reduced volume $\frac{V}{V_0}$ with the mean volume $V_0$ and $y_{\rm sp} = \frac{V_{\rm sp}}{V_0}$. $V_{\rm sp}$ is the critical volume for superparamagnetism which is given by $V_{\rm sp} = \frac{25k_{\rm B}T}{K}$. $M_{\rm sp}(y,h)$ and $M_{\rm B}(h)$ are the reduced magnetization for the superparamagnetic and blocked particles, respectively. It is known that $M_{\rm sp}(h,y) = m_{\rm s}L(2\sigma yh)$, where the Langevin function $L(x) = \coth(x) - \frac{1}{x}$. Usually such an anisotropic nanomagnetic system follows a log–normal distribution of particle size, i.e.

$$f(y) = \frac{1}{\sqrt{2\pi}\gamma y}\exp\Big[-\frac{(\ln y)^2}{2\gamma^2}\Big], \quad (15)$$

where $\gamma$ is the dispersion of the corresponding distribution. For the numerical integration, we have used the following parameters: $\gamma = 0.8$, $V_0 = \exp(-\gamma^2/2)$, and average blocking temperature, $\langle T_{\rm B}\rangle = 15.5$ K, [32]. $T$ is measured in units of $\langle T_{\rm B}\rangle$ and $h$ is measured in units of $m_{\rm s}B/K$.

Numerical integration programs in FORTRAN are performed to calculate the magnetization for the monodispersive and the polydispersive system by using equations (13) and (14), respectively. Static magnetic susceptibility of the polydispersive system is defined as

$$\chi_{\rm pol} = \frac{\partial M_{\rm pol}}{\partial B}. \quad (16)$$

Now, we have defined our system and other essential thermodynamic functions. In the next two sections, we analyse the thermodynamic behaviour of such a magneto-anisotropic nanomagnetic system.

## 4. Energy barrier and equilibrium angle

In this section, we discuss the behaviour of the magnetic potential energy as a function of several parameters used in the Hamiltonian of the present nanomagnetic system. The variation of equilibrium angle, $\theta$, between the magnetic moment and the easy axis of magnetization as a function of $h$ is also studied in this section.

### *4.1. Energy barrier*

One can rewrite equation (4) as follows:

$$U(\theta,\phi) = \frac{\beta H(\theta,\phi)}{\sigma} = \sin^2\theta - 2h \times (\cos\alpha\cos\theta + \sin\alpha\sin\theta\cos\phi), \quad (17)$$

where $\beta = \frac{1}{k_{\rm B}T}$. The stationary points for equation (17) occur for $\phi = 0$ and $\pi$. The stationary point for $\phi = \pi$ corresponds to a maximum, so it is of no physical interest. On the other hand, the stationary point $\phi = 0$ corresponds to maxima at $\theta_{\rm m}$ and minima at $\theta_1$ and $\theta_2$. One can determine two equilibrium directions of the magnetization associated with polar angles $\theta_1$ and $\theta_2$ (lying in the $x$–$z$ plane) from the following condition:

$$\frac{\partial U}{\partial\theta} = 0, \qquad \frac{\partial^2 U}{\partial\theta^2} > 0, \quad (18)$$

and the saddle point is determined by

$$\frac{\partial U}{\partial\theta} = 0, \qquad \frac{\partial^2 U}{\partial\theta^2} < 0. \quad (19)$$

On the other hand, one can determine the critical value of the ratio of field to barrier height ($h_{\rm c}$) at which the potential loses its bistable character by using the following condition:

$$\frac{\partial U}{\partial\theta} = 0 = \frac{\partial^2 U}{\partial\theta^2}. \quad (20)$$

Using equation (20), one can easily show that [33]

$$h_{\rm c} = \frac{1}{\left(\cos^{\frac{2}{3}}\alpha + \sin^{\frac{2}{3}}\alpha\right)^{\frac{3}{2}}}. \quad (21)$$

One can rewrite equation (21) as follows:

$$(1-h_{\rm c}^2)^3 - \tfrac{27}{4}h_{\rm c}^4\sin^2 2\alpha = 0. \quad (22)$$

It can be shown that $|h_{\rm c}|$ lies in the range $0.5 \leqslant |h_{\rm c}| \leqslant 1$. $h_{\rm c} = 1$ occurs for $\alpha = 0$ or $\frac{\pi}{2}$, whereas $h_{\rm c} = \frac{1}{2}$ can be seen for $\alpha = \frac{\pi}{4}$. It is very unlikely that one can derive all the derivatives and hence the barrier heights ($B_1$ and $B_2$) for arbitrary $\alpha$. It is easy to derive barrier heights and to know the nature of the potential for some particular values of $\alpha$. For $\alpha = 0$, $B_1 = \sigma(1+h)^2$ and $B_2 = \sigma(1-h)^2$. Thus the potential has the asymmetric bistable form as shown in figure 2(a). On the other hand, this asymmetric potential becomes symmetric and the barrier height becomes $B_1 = B_2 = \sigma(1-h)^2$ for $\alpha = \frac{\pi}{2}$, $\phi = 0$ (see figure 2(c)). Again for $\alpha = \frac{\pi}{4}$, the potential becomes asymmetric bistable below $h = 0.5$ (see figure 2(b)) and the barrier heights become [22]

$$B_1 = 2\sigma\sqrt{(1/2) - (h^2/2) - h\sqrt{(h^2/4) + (1/2)}} \times \left(\sqrt{(h^2/4) + (1/2)} - 3h/2\right)$$

and

$$B_2 = B_1/2 + \sigma\sqrt{(1/2) - (h^2/2) + h\sqrt{(h^2/4) + (1/2)}} \times \left(\sqrt{(h^2/4) + (1/2)} + 3h/2\right).$$

For $\alpha = \pi$, one can show that $B_1 = \sigma(1-h)^2$ and $B_2 = \sigma(1+h)^2$ and is just the opposite of the case for $\alpha = 0$ (see figure 2(d)). In general the potential retains its asymmetric bistable character for $0 < h < h_{\rm c}$ and $\alpha \neq \frac{\pi}{2}$.

It is evident from figure 2 that the potential energy of this nanomagnetic system has two minima separated by a maxima if and only if $h$ is less than a certain critical value ($h_{\rm c}$) which varies from 0.5 for $\alpha = \frac{\pi}{4}$ to 1.0 for $\alpha = 0, \frac{\pi}{2}$. So, the system consists of two potential barriers $B_1$ and $B_2$ which are, in general, unequal except for the case of $\alpha = \frac{\pi}{2}$. If $h > h_{\rm c}$ the bistable character of the potential disappears and the system has only a single maxima or a single minima. At $h = h_{\rm c}$, the second minima becomes a point of inflection which is clearly seen in figure 2.

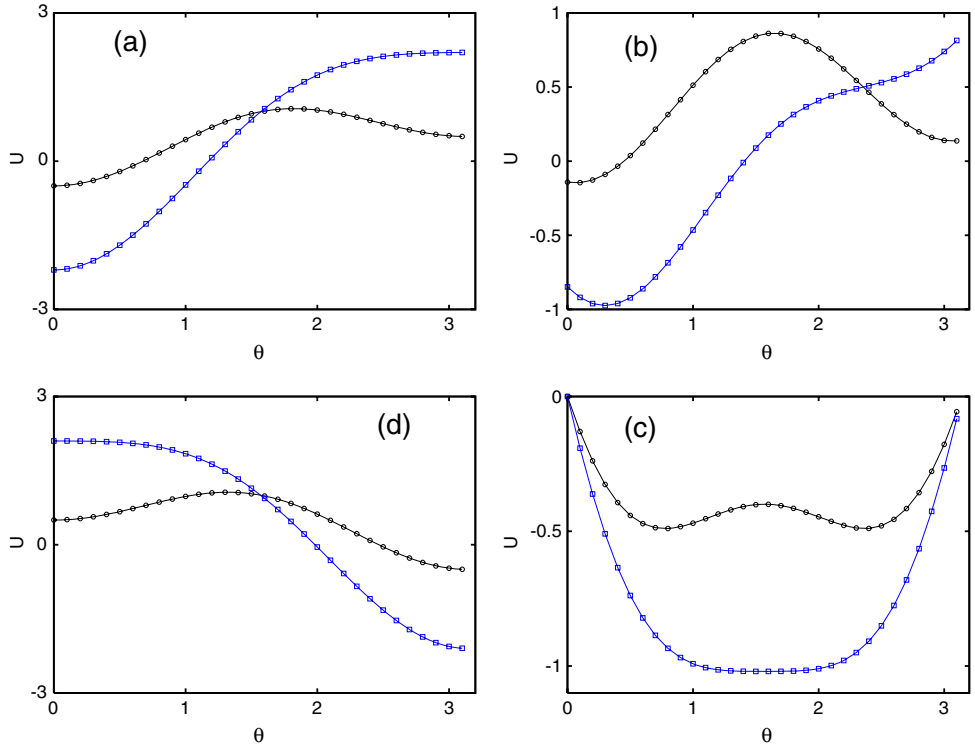


**Figure 2.** Energy is plotted against the angle $\theta$ for different cases with: (a) $\alpha = 0$, $\phi = 0$; $h = 0.25$ (black circle) and $h = 1.1$ (blue square); (b) $\alpha = \frac{\pi}{4}$, $\phi = 0$; $h = 0.1$ (black circle) and $h = 0.6$ (blue square); (c) $\alpha = \frac{\pi}{2}$, $\phi = 0$; $h = 0.7$ (black circle) and $h = 1.01$ (blue square); (d) $\alpha = \pi$, $\phi = 0$; $h = 0.25$ (black circle) and $h = 1.1$ (blue square).

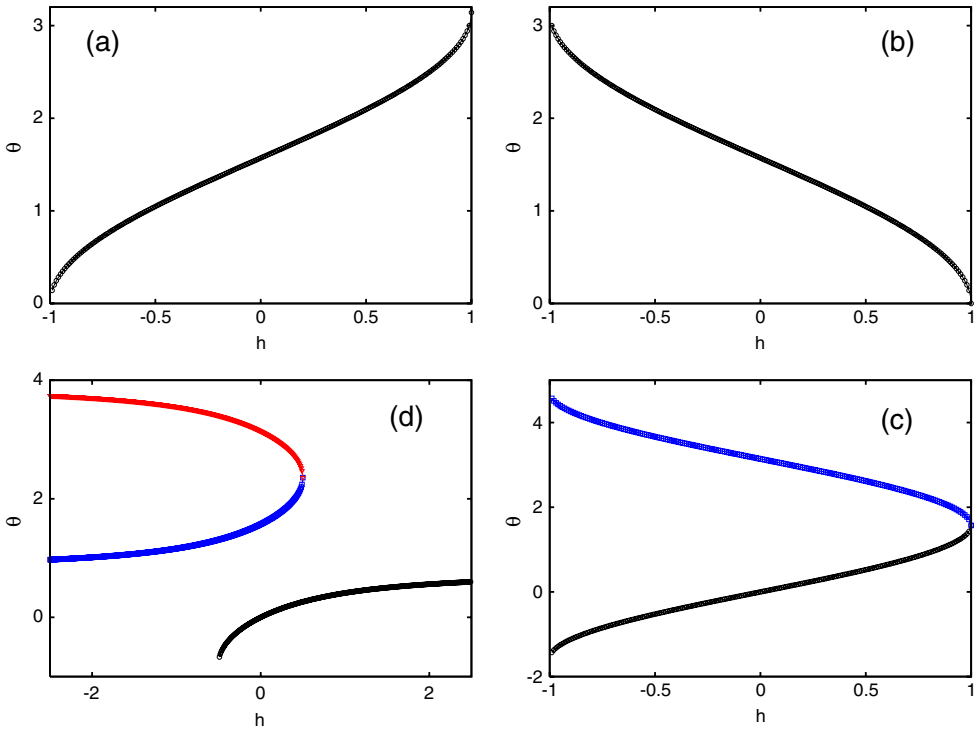


**Figure 3.** Plot of equilibrium angle, $\theta$, versus $h$ with $\phi = 0$ and (a) $\alpha = 0$ for $\theta_{\rm m}$, (b) $\alpha = \pi$ for $\theta_{\rm m}$, (c) $\alpha = \frac{\pi}{2}$; for $\theta_1$ in black circle and $\theta_2$ in blue square, (d) $\alpha = \frac{\pi}{4}$; for $\theta_1$ in black circle, $\theta_{\rm m}$ in blue square and $\theta_2$ in red triangle.

### *4.2. Equilibrium angle*

Here, we are considering a collection of non-interacting magnetic single-domain nanoparticles in the presence of an external magnetic field. The variation of the equilibrium angle between the anisotropy axis and the magnetic moment, $\theta$, versus $h$ for such a collection of non-interacting nanomagnetic

systems is shown in figure 3. Now, using the maxima and minima condition of $U(\theta, \phi)$ as defined by equations (18) and (19), one can obtain the equilibrium angle for the magnetization direction in the $x$–$z$ plane for some specific values of $\alpha$. Finally, the expression for the equilibrium angle $\theta$ for $\phi = 0$ under different orientations of $\alpha$ is as follows:

(i) for $\alpha = 0$ and $\phi = 0$:

$$\theta_{\rm m} = \cos^{-1}(-h), \theta_{1,2} = 0, \pi \tag{23}$$

i.e. $U(\theta, \phi)$ has minima at $\theta_{1,2} = 0, \pi$ and maxima at $\theta_{\rm m} = \cos^{-1}(-h)$.

(ii) For $\alpha = \frac{\pi}{4}$ and $\phi = 0$, the minima of the potential are at $\theta = \theta_1 = \frac{\pi}{4} - \sin^{-1}(-\frac{h}{2} + \frac{\sqrt{h^2+2}}{2})$; $0 \leqslant \theta_1 \leqslant \frac{\pi}{12}$ and at $\theta = \theta_2 = \frac{5\pi}{4} - \sin^{-1}(\frac{h}{2} + \frac{\sqrt{h^2+2}}{2})$; $\frac{3\pi}{4} \leqslant \theta_2 \leqslant \pi$. On the other hand, the magnetic potential has maxima at $\theta = \theta_{\rm m} = \frac{\pi}{4} + \sin^{-1}(\frac{h}{2} + \frac{\sqrt{h^2+2}}{2})$; $\frac{\pi}{2} \leqslant \theta_{\rm m} \leqslant \frac{3\pi}{4}$ [33].

(iii) For $\alpha = \frac{\pi}{2}$ and $\phi = 0$, $U(\theta, \phi)$ has minima at $\theta = \theta_1 = \sin^{-1}(h)$ and $\theta = \theta_2 = \pi - \sin^{-1}(h)$ and maxima at $\theta = \theta_{\rm m} = \frac{\pi}{2}$.

(iv) and finally for $\alpha = \pi$ and $\phi = 0$ one can show that minima of the magnetic potential are at $\theta = \theta_{1,2} = 0, \pi$ and maxima at $\theta = \theta_{\rm m} = \cos^{-1}(h)$.

In figure 3, we plot these solutions as a function of $h$. Figure 3(a) shows that $\theta_{\rm m}$ for $\alpha = 0; \phi = 0$ increases from 0 to 3.0 as $h$ is altered from $-1$ to $+1$. On the other hand, $\theta_{\rm m}$ for $\alpha = \pi; \phi = 0$ decreases from 3.0 to 0 as $h$ is varied from $-1$ to $+1$ (see figure 3(b)). From figure 3(c), it is evident that, as $h$ is varied from $-1$ to $+1$, $\theta_1$ increases from $-\frac{\pi}{2}$ to $\frac{\pi}{2}$ (black filled circle) and $\theta_2$ decreases from $\frac{3\pi}{2}$ to $\frac{\pi}{2}$ (blue filled square). It is seen from figure 3(d) that $\theta_1$ (black filled circle) and $\theta_{\rm m}$ (blue filled square) increases monotonically to a maximum value of $\frac{\pi}{12}$ and $\frac{3\pi}{4}$, respectively, at $h = 0.5$; on the other hand, $\theta_2$ decreases monotonically to a minimum value of $\frac{3\pi}{4}$ at $h = 0.5$ (red filled triangle).

## 5. Magnetization and susceptibility

Magnetization and susceptibility are the most fundamental thermodynamical quantities of non-interacting magnetic nanoparticles with axially symmetric magnetic-anisotropy. In this section, we analyse the variation of these two fundamental quantities with temperature and externally applied magnetic field. The differences and similarities of the magnetization and susceptibility between the ideal superparamagnetic system and a collection of non-interacting anisotropic monodomain particles are presented here.

### *5.1. Magnetization*

The magnetization along the direction of the external magnetic field for classical spins with axially symmetric magnetic anisotropy is defined by equation (13). We illustrate this magnetization as a function of $\xi$ using equation (13) for a system of identical non-interacting monodomain particles for different values of $\sigma$ in figure 4. One can easily observe that magnetization curves differ from the Langevin law in all cases.

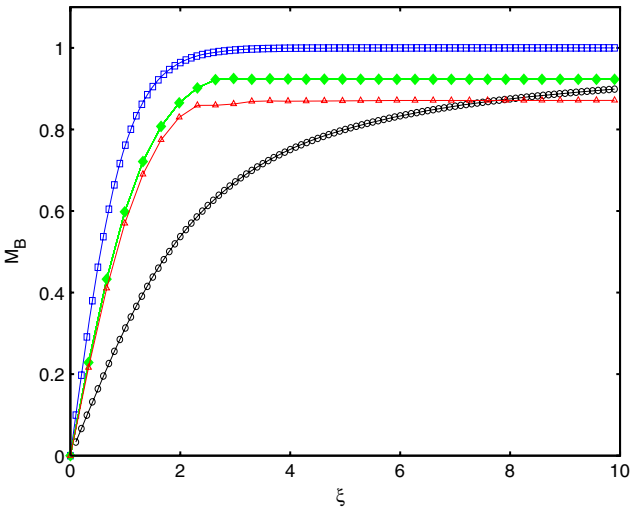


**Figure 4.** Reduced magnetization for the monodispersive system as a function of $\xi$ for various values of the anisotropy parameter, $\sigma$. The black circle and blue square represent Langevin ($\sigma = 0$) and Ising ($\sigma \gg 1$) cases, respectively. Green square and red upward triangle represent magnetization curves for $\sigma = 5.0$ and $\sigma = 2.0$, respectively.

As $\sigma$ decreases, the difference vanishes and, with the increase of $\sigma$, the magnetization curves become closer to the Ising case. In the limits of high and low field, $\xi$, magnetization, $M_{\rm B}$, approaches the Langevin value. The largest influence of anisotropy can be observed in the intermediate-field regime. This confirms the non-Langevin behaviour of a collection of non-interacting magneto-anisotropic single-domain particles. In figure 5, we show the variation of magnetization with reduced temperature, $T_{\rm r} = \frac{T}{\langle T_{\rm B} \rangle}$, for two different values of $h$. Here $\langle T_{\rm B} \rangle$ is the average blocking temperature of the system [34]. For convenience, we also plot the magnetization curves for the Ising and Langevin cases. It is clear that magnetization versus temperature curves for the anisotropic magnetic nanoparticle system show a maximum near $T_{\rm r} = 1.0$, unlike the Ising and Langevin cases. This maximum can be interpreted as follows. From equation (14), one can observe that $M_{\rm pol}$ has two parts, the superparamagnetic contribution and the blocked particle contribution. As the temperature increases the fraction of the superparamagnetic contribution increases until the temperature reaches the blocking temperature. Now, above this blocking temperature at which the maximum in magnetization is observed, the system usually becomes superparamagnetic and magnetization decreases rapidly with the increase of temperature due to thermal agitation. Thus, in equilibrium and for $h < h_{\rm c}$, one can observe a maximum in magnetization for the polydisperse magneto-anisotropic nanoparticle system. One can observe that the maximum of the peak is not exactly at $T_{\rm r} = 1.0$, but with the increase of field it shifts to a lower relative temperature, i.e. maxima are seen at $T_{\rm r} = 0.89$ and at $T_{\rm r} = 0.83$ for $h = 0.2$ and $h = 0.5$, respectively. Also one can notice that, as the field increases, the peak becomes broader.

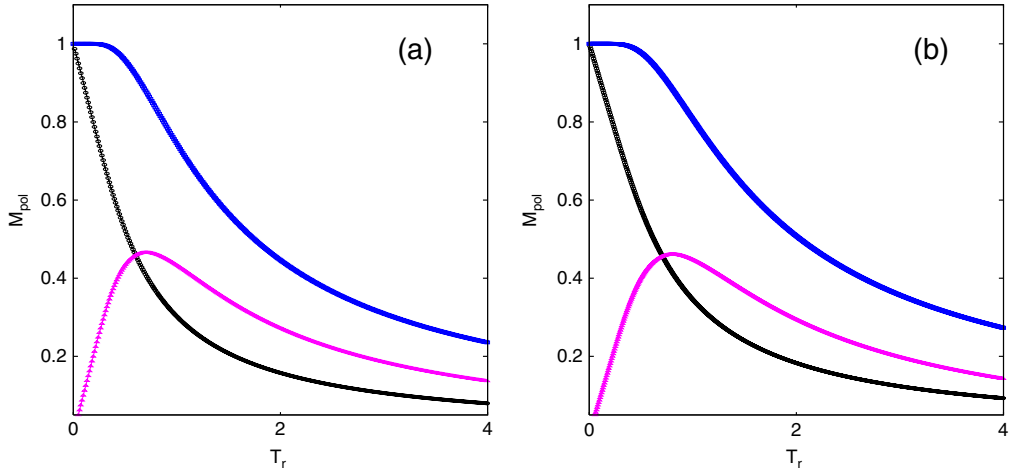


**Figure 5.** Reduced magnetization along the external field axis for a collection of non-interacting, monodomain and polydispersive nanoparticles as a function of reduced temperature. The black circle, blue square and pink upward triangle represent Langevin, Ising and magneto-anisotropic cases, respectively: (a) $h = 0.2$ and (b) $h = 0.5$.

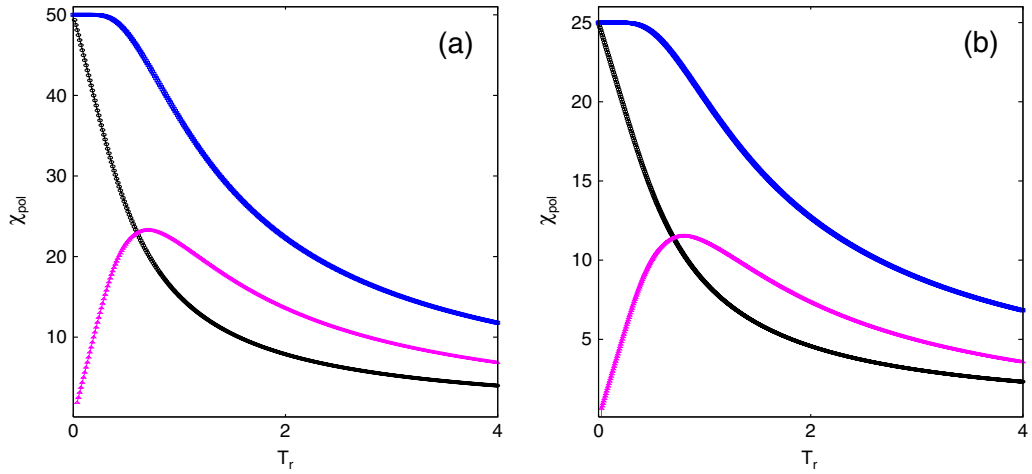


**Figure 6.** Static magnetic susceptibility along the external field axis for a collection of non-interacting, monodomain and polydispersive nanoparticles as a function of reduced temperature. The black circle, blue square and pink upward triangle represent Langevin, Ising and magneto-anisotropic cases, respectively: (a) $h = 0.2$ and (b) $h = 0.5$.

### *5.2. Susceptibility*

In order to demonstrate the effect of magnetocrystalline anisotropy on the thermodynamical quantities, we demonstrate the behaviour of susceptibility of the non-interacting nanoparticles in the presence of an external magnetic field. We plot the susceptibility and inverse susceptibility curves with respect to temperature for different orientations in $\alpha$ between the anisotropy axis and external field in figures 6 and 7, respectively. Again, susceptibility shows a maximum at finite temperatures ($T_r = 0.89$ and $T_r = 0.83$) for $h = 0.2$ and $h = 0.5$, respectively. Also, as the field increases the peak of the susceptibility curves becomes more broad. In order to demonstrate the effect of magnetocrystalline anisotropy, we illustrate the behaviour of inverse susceptibility of the non-interacting nanoparticles with reduced temperature in the presence of an external magnetic field for different orientations of $\alpha$ between the anisotropy axis and external field in figure 7. For $\alpha = 0, \phi = 0$ (in black circle), one observes a susceptibility curve resembling a system with ferromagnetic-like interaction and it follows the Curie–Weiss law. The same kind of ferromagnetic-like coupling is prevalent for $\alpha = \frac{\pi}{15}$ (orange square) and for $\alpha = \frac{\pi}{10}$ (pink upward triangle). This means the zero crossing at the temperature axis occurs at positive values. When the angle between the anisotropy axis and magnetic field is $\alpha = \frac{\pi}{4}$ (red downward triangle), the system resembles paramagnetic behaviour and it follows the simple Curie law. However, for $\alpha = \frac{\pi}{2}$ (blue diamond) and for $\alpha = \frac{\pi}{3}$ (green filled square), a Curie–Weiss antiferromagnetic-like behaviour is observed. By extrapolating one can observe the zero crossing on the temperature axis at negative values. Thus, the extrapolating transition temperature continuously changes from positive values to negative values. From this kind of observation, one can conclude that the anisotropy field acts as a ferromagnetic-, antiferromagnetic- or paramagnetic-like coupling among the magnetic nanoparticles,

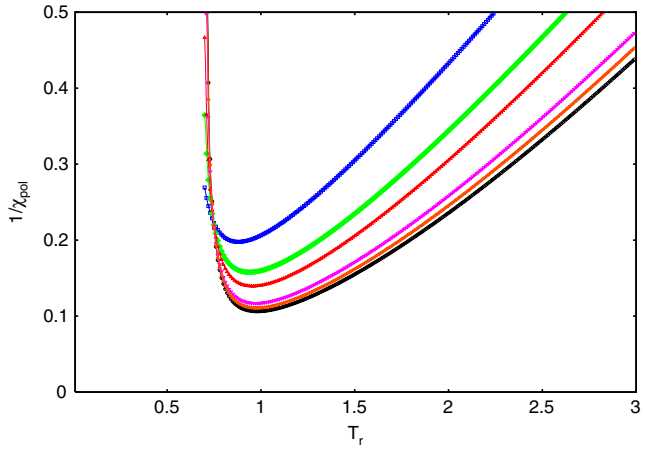


**Figure 7.** Inverse magnetic susceptibilities as a function of reduced temperature. Different curves represent different angles between anisotropy axis and external field (for details see text).

depending on the relative angle between the anisotropy axis and the external field. The net effect of the anisotropy field resembles a continuous transition from a ferromagnetic- to an antiferromagnetic-like coupling.

## 6. Conclusions

In conclusion, we have confirmed that a collection of non-interacting magneto-anisotropic particles cannot be described with the help of the classical Langevin theory, i.e. their thermodynamic equilibrium magnetization and static magnetic susceptibility cannot be described by the Langevin function and its derivative. This deviation is due to the presence of magnetocrystalline anisotropy. The effect of magnetocrystalline anisotropy is explored through magnetization curves and susceptibility curves. The variation of inverse susceptibility with temperature shows paramagnetic, ferromagnetic and antiferromagnetic coupling behaviour for different orientations of $\alpha$. We also present a mechanical analogy for a system in 3D as a frictionless particle moving on a sphere rotating about its vertical diameter. This study reveals the essential role of the magnetocrystalline anisotropy energy in interpreting equilibrium magnetization and susceptibility of a collection of non-interacting single-domain nanomagnetic particles.

## Appendix

In this appendix, we discuss the mechanical isomorph of the nanomagnetic system. We consider a rigid sphere of radius $R_s$ rotating along its vertical diameter at angular frequency $\omega$ with a frictionless particle of mass $M$ free to move on the surface of the sphere as shown in figure A.1. In the rotating coordinate frame $(r, \theta, \phi)$ attached to the rigid sphere, in addition to the gravitational force on the mass $M\vec{g}_a = Mg_a \cos\theta \hat{e}_r - Mg_a \sin\theta \hat{e}_\theta$, a fictitious centrifugal force $\vec{f}$ is acting on the particle and is given by $\vec{f} = M\omega^2 r \sin^2\theta \hat{e}_r + M\omega^2 r \sin\theta \cos\theta \hat{e}_\theta$. An external field $\vec{F}$ is acting on the azimuthal plane such that $\vec{F} = F \sin\phi \hat{e}_\phi$. Now, the kinetic energy of the particle is given by

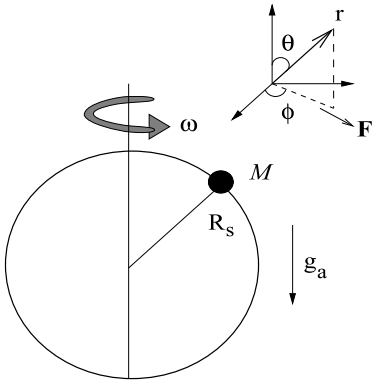


**Figure A.1.** Mechanical rotating system analogous to the nanomagnetic system.

$$T = \tfrac{1}{2}M(\dot{r}^2 + r^2\dot{\theta}^2 + r^2 \sin^2\theta\dot{\phi}^2). \tag{24}$$

The potential energy of the particle consists of three parts $U = U_{g_a} + U_c + U_e$, where $U_{g_a}$ is coming from the gravitational force field part, $U_c$ is the fictitious centrifugal part and $U_e$ is the external field part. Now, one can easily find out the three parts of the effective potential energy as follows:

$$\begin{aligned} U_{g_a} &= -Mg_a R_s \cos\theta \\ U_c &= \tfrac{1}{2}M\omega^2 R_s^2 \cos^2\theta - \tfrac{1}{4}M\omega^2 R_s^2 \\ U_e &= F R_s \sin\theta \cos\phi. \end{aligned} \tag{25}$$

Thus the Lagrangian of the system becomes

$$\begin{aligned} \mathcal{L} = {} & \tfrac{1}{2}M(\dot{r}^2 + r^2\dot{\theta}^2 + r^2 \sin^2\theta\dot{\phi}^2) + Mg_a R_s \cos\theta \\ & + \tfrac{1}{4}M\omega^2 R_s^2 - \tfrac{1}{2}M\omega^2 \cos^2\theta - F R_s \sin\theta \cos\phi. \end{aligned} \tag{26}$$

Now, the effective potential energy which includes the effect of gravity, rotation of the system and the external field force $\vec{F}$ is given by

$$\begin{aligned} u = \frac{U}{Mg_a R_s} = {} & -\cos\theta - \frac{\omega^2 R_s}{4g_a} \\ & + \frac{\omega^2 R_s}{2g_a}\cos^2\theta + \frac{F}{Mg_a}\sin\theta\cos\phi. \end{aligned} \tag{27}$$

Comparing equations (3) and (27) one can easily understand the analogy between the mechanical system and the magnetic nanoparticle system. The centripetal acceleration plays the role of the magnetic anisotropy, whereas the combined effect of the external field $\vec{F}$ and the gravity field is equivalent to the external magnetic field.

## References

[1] Dormann J L, Fiorani D and Tronc E 1997 *Adv. Chem. Phys.* **98** 283
[2] Puntes V F, Krishnan K M and Alivisatos A P 2001 *Science* **291** 2115
[3] Frankel J and Dorfman J 1930 *Nature* **126** 274
[4] Sun S, Murray C B, Weller D, Folks L and Moser A 2000 *Science* **287** 1989

[5] Bean C P and Livingstone J D 1959 *J. Appl. Phys.* **30** 120s
Jacobs I S and Bean C P 1963 *Magnetism* vol III ed G T Rado and H Suhl (New York: Academic)
[6] Lederman M, Schultz S and Osaki M 1994 *Phys. Rev. Lett.* **73** 1986
[7] Jamet M, Wernsdorfer W, Thirion C, Mailly D, Dupuis V, Mélinon P and Pérez A 2001 *Phys. Rev. Lett.* **86** 4676
[8] Kent A D, Shaw T M, von Molnár S and Awschalom D D 1993 *Science* **262** 1250
[9] Kent A D, von Molnár S, Gider S and Awschalom D D 1994 *J. Appl. Phys.* **76** 6656
[10] Dormann J L, Fiorani D and Tronc E 1997 *Adv. Chem. Phys.* **98** 283
[11] Kittel C 1946 *Phys. Rev.* **70** 965
[12] Aharoni A 1964 *Phys. Rev.* A **135** 447
[13] Néel L 1949 *Ann. Geophys.* **5** 99
[14] Brown W F Jr 1963 *Phys. Rev.* **130** 1677
[15] Stoner E C and Wohlfarth E P 1948 *Phil. Trans. R. Soc.* **240** 599
Stoner E C and Wohlfarth E P 1991 *IEEE Trans. Magn.* **27** 3475
[16] West F G 1961 *J. Appl. Phys.* **30** 249s
[17] Müller K and Thurley F 1973 *Int. J. Magn.* **5** 203
[18] Hanson M, Johansson C and Mørup S 1993 *J. Phys.: Condens. Matter* **5** 725
[19] Williams H D, O'Grady K, Hilo M E and Chantrell R W 1993 *J. Magn. Magn. Mater.* **122** 129
[20] García-Palacios J L 2000 *Advances in Chemical Physics* vol 112 ed I Priogogine and S A Rice (New York: Wiley) p 1
[21] Respaud M 1999 *J. Appl. Phys.* **86** 556
[22] Pfeiffer H 1990 *Phys. Status Solidi* a **122** 377
[23] Pfeiffer H 1990 *Phys. Status Solidi* a **120** 233
[24] Madsen D E, Mørup S and Hansen M F 2006 *J. Magn. Magn. Mater.* **305** 95
[25] Vargas P, Altbir D, Knobel M and Laroze D 2002 *Europhys. Lett.* **58** 603
[26] Vargas P and Laroze D 2004 *J. Magn. Magn. Mater.* **272** e1345
[27] Wiekhorst F, Shevchenko E, Weller H and Kötzler J 2003 *Phys. Rev.* B **67** 224416
[28] Shevchenko E V, Talapin D V, Rogach A L, Kronowski A, Haase M and Weller H 2002 *J. Am. Chem. Soc.* **124** 11480
[29] Bandyopadhyay M and Bhattacharya J 2006 *J. Phys.: Condens. Matter* **18** 11309
[30] Chakraverty S, Bandyopadhyay M, Chatterjee S, Dattagupta S, Frydman A, Sengupta S and Sreeram P A 2005 *Phys. Rev.* B **71** 054401
[31] Sun Y, Salamon M B, Garnier K and Averback R S 2004 *Phys. Rev. Lett.* **93** 139703
[32] El-Hilo M, O'Grady K and Chantrell R W 1992 *J. Magn. Magn. Mater.* **117** 21
[33] Coffey W T, Crothers D S F, Dormann J L, Geoghegan L J, Kalmykov Yu P, Waldron J T and Wickstead A W 1995 *Phys. Rev.* B **52** 15951
[34] Bandyopadhyay M and Dattagupta S 2006 *Phys. Rev.* B **74** 214410